Sensors and Materials, Vol. 37, No. 2 (2025) 593–598
MYU Tokyo

S & M 3939

Radioluminescence Properties of Tb-doped $Ca_3TaGa_3Si_2O_{14}$ Single Crystals

Ryosei Takahashi,* Kai Okazaki, Daisuke Nakauchi,
Takumi Kato, Noriaki Kawaguchi, and Takayuki Yanagida

Nara Institute of Science and Technology (NAIST), 8916-5 Takayama-cho, Ikoma, Nara 630-0192, Japan

(Received October 25, 2024; accepted December 13, 2024)

Keywords: scintillator, phosphor, radiation detection, CTGS

Tb-doped $Ca_3TaGa_3Si_2O_{14}$ (CTGS) single crystals with different concentrations were synthesized to evaluate their photoluminescence and radioluminescence properties. All the samples showed emissions due to the 4f–4f transitions of Tb^{3+}. The 2% Tb-doped sample showed the highest quantum yield of 16.4% upon excitation at 350 nm. Decay curves demonstrated decay time constants of 2.0–2.1 ms, which were the typical values for the 4f–4f transitions of Tb^{3+}.

1. Introduction

Scintillators are phosphors that immediately convert the energy of ionizing radiations into low-energy photons.[1–5] They have been applied in many fields such as security screening,[6,7] medical imaging,[8,9] well logging,[10,11] and high-energy physics.[12,13] Various materials have been used depending on the types and energies of the radiation and application: single crystal,[14–17] glass,[18–20] and ceramic.[21–23]

A Tb-doped Gd_2O_2S (Tb:GOS) ceramic has been applied in, for example, flat panel detectors for X-ray detection[24] because of its large Z_{eff} (61.1) and high radioluminescence (RL) intensity.[25] In addition, the main emission peak of Tb is observed at 540 nm, which is appropriate for the sensitivity of conventional photodetectors such as Si photodiodes. However, GOS suffers from low X-ray spatial resolution because of light scattering caused by the large particle sizes and grain boundaries of ceramics.[26] Although the melting point of GOS is 2265 °C,[27] the synthesis of the bulk single crystal is difficult owing to S^{2-} loss caused by thermal decomposition and evaporation. Therefore, alternative materials with large Z_{eff}, high RL intensity, and high transparency are desired.

$Ca_3TaGa_3Si_2O_{14}$ (CTGS) single crystals with Z_{eff} of 51 were focused on as a host material because large crystals of CTGS can be easily grown because they have a low melting point (1300–1500 °C).[28] For this reason, CTGS single crystals are attractive for scintillator applications. Here, Tb was selected as a luminescence center imitating Tb:GOS. In addition to the advantages of compatibility between the emission wavelengths and wavelength sensitivities

*Corresponding author: e-mail: takahashi.ryosei.tn7@naist.ac.jp
https://doi.org/10.18494/SAM5435

ISSN 0914-4935

of Si-based detectors, rare-earth elements can be substituted at Ca sites because the ionic radius of a rare-earth ion in 8-hold coordination (Tb: 1.04 Å) is close to that of Ca^{2+} in 8-hold coordination (1.12 Å).[29,30] This close match of ionic radius minimizes lattice distortion, promoting efficient energy transfer and enhancing luminescence properties. On the basis of this design, Tb-doped CTGS (Tb:CTGS) single crystals were successfully synthesized, and their photoluminescence (PL) and RL properties were evaluated.

2. Materials and Methods

0.5, 1, 2, and 3 at% (with respect to Ca) Tb:CTGS single crystals were synthesized by the floating zone (FZ) method. CaO (99.99%), Ta_2O_5 (99.99%), Ga_2O_3 (99.99%), SiO_2 (99.999%), and Tb_4O_7 (99.99%) powders used as raw materials were homogeneously mixed with a mortar and pestle. The synthesis method followed the procedures for Nd-doped CTGS.[31] Part of the synthesized samples were crushed and mechanically polished. X-ray diffraction (XRD) measurements were conducted with a diffractometer (MiniFlex600, Rigaku). PL 3D spectra and PL quantum yields (*QY*s) were measured using Quantaurus-QY (C11347, Hamamatsu Photonics), and PL decay curves were evaluated using Quantaurus-τ (C11367, Hamamatsu Photonics). In terms of RL properties, X-ray-induced RL spectra and decay curves were investigated using our original devices.[32,33]

3. Results and Discussion

Figure 1 shows the appearance of the polished Tb-doped CTGS samples. All the samples appeared colorless and transparent. The length and thickness respectively were 4–6 mm and 0.8 mm. Figure 2 displays XRD patterns of the prepared samples and a reference of CTGS [(Crystallography Open Database (COD)]: 8100499). All the diffraction patterns of the prepared samples matched with the reference data and no impurity phases were confirmed. Therefore, all the samples had a single phase of CTGS belonging to the trigonal system with a space group of *P*321.[34] The peak intensity ratio of the 0.5% Tb-doped sample differed from those of the other

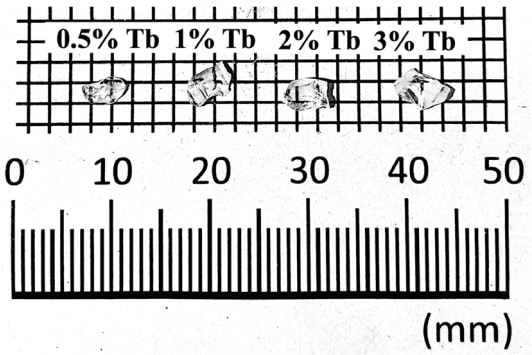

Fig. 1. Appearance of Tb-doped CTGS.

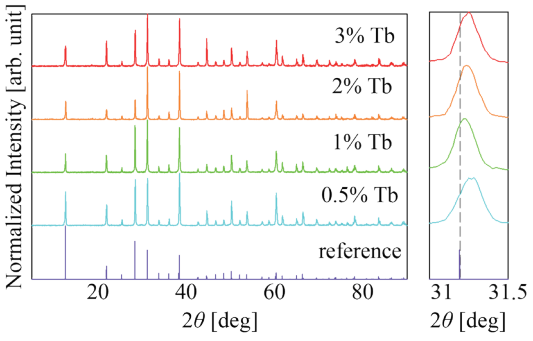

Fig. 2. (Color online) XRD patterns of Tb:CTGS and reference (COD: 8100499) at (left) 5–90 degrees and (right) 30.5–31.5 degrees.

prepared samples. The powders used were prepared by crushing with a mortar and pestle; hence, heterogeneity in the dominant planes would appear. When comparing the peaks with the those of the reference pattern, the peaks of all the samples were shifted to larger angles. This suggests that Tb^{3+} in the 8-hold coordination was substituted at Ca^{2+} sites since the ionic radii of Tb^{3+} and Ca^{2+} were similar (1.04 and 1.12 Å, respectively).

Figure 3 displays the PL 3D spectra of the Tb:CTGS samples. All the samples showed several emission peaks at 350–650 nm, which were attributed to the 4f–4f transitions of Tb^{3+} because similar emission peaks were confirmed at the same wavelengths in the PL spectra of the other Tb-doped phosphors.[35,36] The specified transitions are listed in Fig. 3. No intrinsic luminescence was observed in any of the Tb-doped samples. Undoped CTGS has been reported to show luminescence at 440 nm under excitation at 200–250 nm.[31] Its absence could be attributed to the low intensity of the intrinsic luminescence rather than that of Tb^{3+}. *QY*s of the 0.5, 1, 2, and 3% Tb-doped samples respectively were 11.2, 12.8, 16.4, and 9.8% when monitored at 370–800 nm under excitation at 350 nm. The decrease in *QY* of the 3% Tb-doped sample would be due to concentration quenching.

Figure 4 shows the PL decay curves of the prepared Tb-doped samples. The PL decay curves were obtained by monitoring at 550 nm under excitation at 340 nm and approximated by the sum of two exponential functions. The fast component was due to an instrumental response function (IRF), which was caused by the excitation source. The decay time constants of the slow components were 2.0–2.1 ms, which were typical values for the 4f–4f transitions of Tb^{3+}.[37,38]

Figure 5 displays the X-ray-induced RL spectra of the prepared samples. Slightly broad peaks were confirmed at 300–550 nm, and they are thought to originate from the intrinsic luminescence because the emission was also observed in an RL spectrum of undoped CTGS.[31] All the samples showed several sharp emission lines at 390, 420, 440, 460, 480, 490, 550, 590, and 610 nm, which were the same as the wavelengths in PL spectra (Fig. 3). Furthermore, almost the same spectral features were confirmed in RL spectra of some other Tb-doped scintillators.[37,39–41] Therefore, the emission originated from the 4f–4f transitions of Tb^{3+}.

Figure 6 shows X-ray-induced RL decay curves of the Tb-doped CTGS samples. The decay curves were approximated using the sum of three exponential functions. The fastest component

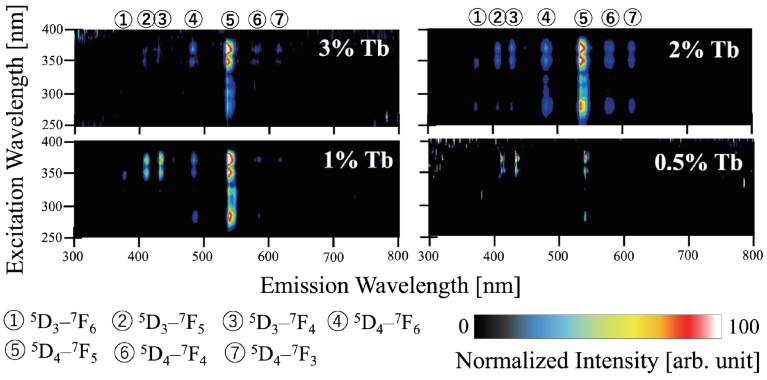

Fig. 3. (Color online) PL 3D spectra of Tb:CTGS. The horizontal and vertical axes show the emission and excitation wavelengths, respectively.

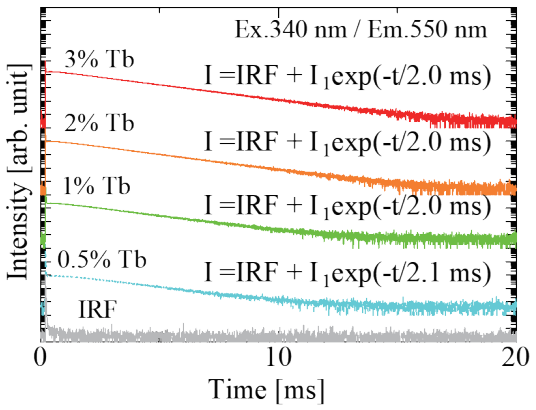

Fig. 4. (Color online) PL decay curves of Tb:CTGS.

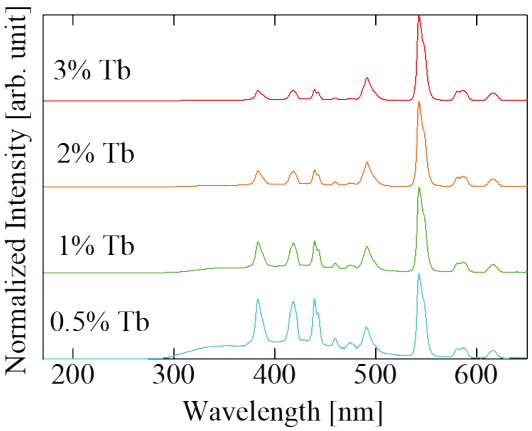

Fig. 5. (Color online) X-ray-induced RL spectra of Tb:CTGS.

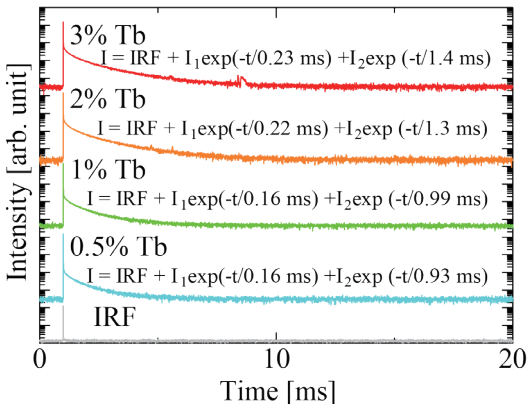

Fig. 6. (Color online) X-ray-induced RL decay curves of Tb:CTGS.

was attributed to an IRF. The second fastest component had decay time constants of 0.16–0.23 ms, and the slowest components showed decay times of 0.93–1.4 ms. The decay times of the two slow components were consistent with the 4f–4f transitions of Tb^{3+}.[36,37] The different decay times can be due to the different electronic transitions.[42] During the measurement, emission signals at 160–650 nm, covered by wavelength sensitivities of the photomultiplier tube used, were accumulated. As a result, multiple components were observed, unlike the PL decay curves shown in Fig. 4. The decay times of the slowest components were shorter than PL decay times, likely owing to the high excitation density of X-rays, which increase nonradiative relaxation probabilities through interactions among numerous excited electrons.[43]

4. Conclusions and Future Prospects

0.5, 1, 2, and 3% Tb:CTGS single crystals were synthesized by the FZ method. Under UV or X-ray excitation, they showed several emission lines due to the 4f–4f transitions of Tb^{3+} at 350–650 nm, and *QY* of the 2% Tb-doped sample was 16.4%. The RL decay curves of the samples

were approximated using two exponential components (0.16–0.23 and 0.93–1.4 ms), confirming the origin to be the 4f–4f transitions of Tb^{3+}. From these results, RL properties due to the electronic transitions of Tb^{3+} were closely observed in Tb-doped CTGS. However, *QY* was relatively low, leading to low RL efficiencies. CTGS is known to be substituted by other alkali-earth elements such as Sr and Ba at Ca sites. By substituting the Ca sites with other alkali-earth metal elements, the density of the host is increased, and better Tb-doped scintillators with high *QY*s and RL efficiencies may be developed.

Acknowledgments

This work was supported by MEXT Grants-in-Aid for Scientific Research A (22H00309), Scientific Research B (23K21827,23K25126 and 24K03197), Exploratory Research (22K18997), and Early-Career Scientists (23K13689). Suzuki Foundation, Asahi Glass Foundation, and Konica Minolta Science and Technology Foundation are also acknowledged.

References

1 M. J. Weber: J. Lumin. **100** (2002) 35.
2 C. L. Melcher: Nucl. Instrum. Methods Phys. Res., Sect. A **537** (2005) 6.
3 C. W. E. van Eijk: Nucl. Instrum. Methods Phys. Res., Sect. A **392** (1997) 285.
4 T. Yanagida, T. Kato, D. Nakauchi, and N. Kawaguchi: Jpn. J. Appl. Phys. **62** (2023) 010508.
5 T. Yanagida: Proc. Jpn. Acad., B **94** (2018) 75.
6 J. Glodo, Y. Wang, R. Shawgo, C. Brecher, R. H. Hawrami, J. Tower, and K. S. Shah: Phys. Procedia **90** (2017) 285.
7 V. D. Ryzhikov, A. D. Opolonin, P. V. Pashko, V. M. Svishch, V. G. Volkov, E. K. Lysetskaya, D. N. Kozin, and C. Smith: Nucl. Instrum. Methods Phys. Res., Sect. A **537** (2005) 424.
8 P. Lecoq: Nucl. Instrum. Methods Phys. Res., Sect. A **809** (2016) 130.
9 C. Ronda, H. Wieczorek, V. Khanin, and P. Rodnyi: ECS J. Solid State Sci. Technol. **5** (2016) R3121.
10 C. L. Melcher, J. S. Schweitzer, R. A. Manente, and C. A. Peterson: J. Cryst. Growth **109** (1991) 37.
11 T. Yanagida, Y. Fujimoto, S. Kurosawa, K. Kamada, H. Takahashi, Y. Fukazawa, M. Nikl, and V. Chani: Jpn. J. Appl. Phys. **52** (2013) 076401.
12 R. Mao, L. Zhang, and R.-Y. Zhu: IEEE Trans. Nucl. Sci. **55** (2008) 2425.
13 M. Kole, M. Chauvin, Y. Fukazawa, K. Fukuda, S. Ishizu, M. Jackson, T. Kamae, N. Kawaguchi, T. Kawano, M. Kiss, E. Moretti, M. Pearce, S. Rydström, H. Takahashi, and T. Yanagida: Nucl. Instrum. Methods Phys. Res., Sect. A **770** (2015) 68.
14 D. Shiratori, H. Fukushima, D. Nakauchi, T. Kato, N. Kawaguchi, and T. Yanagida: Sens. Mater. **35** (2023) 439.
15 K. Miyazaki, D. Nakauchi, T. Kato, N. Kawaguchi, and T. Yanagida: Sens. Mater. **36** (2024) 515.
16 Y. Endo, K. Ichiba, D. Nakauchi, T. Kato, N. Kawaguchi, and T. Yanagida: Sens. Mater. **36** (2024) 473.
17 T. Kunikata, P. Kantuptim, D. Shiratori, T. Kato, D. Nakauchi, N. Kawaguchi, and T. Yanagida: Sens. Mater. **36** (2024) 457.
18 K. Okazaki, D. Nakauchi, A. Nishikawa, T. Kato, N. Kawaguchi, and T. Yanagida: Sens. Mater. **36** (2024) 587.
19 Y. Takebuchi, A. Masuno, D. Shiratori, K. Ichiba, A. Nishikawa, T. Kato, D. Nakauchi, N. Kawaguchi, and T. Yanagida: Sens. Mater. **36** (2024) 579.
20 D. Nakauchi, H. Kimura, D. Shiratori, T. Kato, N. Kawaguchi, and T. Yanagida: Sens. Mater. **36** (2024) 573.
21 T. Kato, D. Nakauchi, N. Kawaguchi, and T. Yanagida: Sens. Mater. **36** (2024) 531.
22 D. Nakauchi, F. Nakamura, T. Kato, N. Kawaguchi, and T. Yanagida: Sens. Mater. **35** (2023) 467.
23 T. Kunikata, T. Kato, D. Shiratori, P. Kantuptim, D. Nakauchi, N. Kawaguchi, and T. Yanagida: Sens. Mater. **35** (2023) 491.
24 A. Howansky, A. Mishchenko, A. R. Lubinsky, and W. Zhao: Med. Phys. **46** (2019) 4857.
25 R. Chouikrat, F. Baros, J. C. André, R. Vanderesse, B. Viana, A. L. Bulin, C. Dujardin, P. Arnoux, M. Verelst, and C. Frochot: Photochem. Photobiol. **93** (2017) 1439.

26 K. E. Yorov, S. Nematulloev, B. M. Saidzhonov, M. S. Skorotetcky, A. A. Karluk, B. E. Hasanov, W. J. Mir, T. Sheikh, L. Gutiérrez-Arzaluz, M. E. M. Phielepeit, N. Ashraf, R. H. Blick, O. F. Mohammed, M. Bayindir, and O. M. Bakr: ACS Nano **18** (2024) 20111.
27 G. Xu, H. Qin, T. Huang, F. Liu, and J. Lian: Optoelectron. Adv. Mater. Rapid Commun. **11** (2017) 703.
28 S. Kurosawa, M. Kitahara, Y. Yokota, K. Hishinuma, T. Kudo, O. Buzanov, A. Medvedev, V. I. Chani, and A. Yoshikawa: IEEE Trans. Nucl. Sci. **61** (2014) 339.
29 L. Liu, X. Xin, Q. Chi, X. Ma, X. Fu, Z. Jia, and X. Tao: J. Cryst. Growth **578** (2022) 126428.
30 B. Han, Y. Huang, J. Huang, X. Gong, Y. Lin, Z. Luo, and Y. Chen: J. Lumin. **258** (2023) 119790.
31 K. Okazaki, M. Koshimizu, D. Nakauchi, T. Kunikata, T. Kato, N. Kawaguchi, and T. Yanagida: J. Alloys. Compd. **1008** (2024) 176788.
32 T. Yanagida, K. Kamada, Y. Fujimoto, H. Yagi, and T. Yanagitani: Opt. Mater. **35** (2013) 2480.
33 T. Yanagida, Y. Fujimoto, T. Ito, K. Uchiyama, and K. Mori: Appl. Phys. Express **7** (2014) 062401.
34 X. Fu, E. G. Víllora, Y. Matsushita, Y. Kitanaka, Y. Noguchi, M. Miyayama, K. Shimamura, and N. Ohashi: J. Ceram. Soc. Jpn. **124** (2016) 523.
35 D. Nakauchi, T. Kato, N. Kawaguchi, and T. Yanagida: Sens. Mater. **33** (2021) 2203.
36 P. Kantuptim, T. Kato, D. Nakauchi, N. Kawaguchi, K. Watanabe, and T. Yanagida: Sens. Mater. **35** (2023) 451.
37 Y. Endo, K. Ichiba, D. Nakauchi, H. Fukushima, K. Watanabe, T. Kato, N. Kawaguchi, and T. Yanagida: Solid State Sci. **145** (2023) 107333.
38 H. Kimura, H. Fukushima, K. Watanabe, T. Fujiwara, H. Kato, M. Tanaka, T. Kato, D. Nakauchi, N. Kawaguchi, and T. Yanagida: Sens. Mater. **36** (2024) 507.
39 H. Pan, Q. Liu, X. Chen, X. Liu, H. Chen, T. Xie, W. Wang, Y. Shi, X. Jiang, J. Zhou, Z. Sun, M. Nikl, and J. Li: Opt. Mater. **105** (2020) 109909.
40 D. Nakauchi, K. Watanabe, T. Kato, N. Kawaguchi, and T. Yanagida: Nucl. Instrum. Methods Phys. Res., Sect. B **546** (2024) 165167.
41 N. Kawaguchi, K. Watanabe, D. Shiratori, T. Kato, D. Nakauchi, and T. Yanagida: Sens. Mater. **35** (2023) 499.
42 J. Drabik, R. Kowalski, and L. Marciniak: Sci. Rep. **10** (2020) 11190.
43 T. Yanagida and G. Okada: J. Ceram. Soc. Jpn. **124** (2016) 564.